APL Photonics

RESEARCH ARTICLE | JUNE 17 2024

High-order harmonic generation in liquid crystals

Andrea Annunziata ; Luise Becker ; Marta L. Murillo-Sánchez ; Patrick Friebel ; Salvatore Stagira ; Davide Faccialà ; Caterina Vozzi ; Laura Cattaneo

APL Photonics 9, 060801 (2024)
https://doi.org/10.1063/5.0191184

High-order harmonic generation in liquid crystals

Cite as: APL Photon. 9, 060801 (2024); doi: 10.1063/5.0191184
Submitted: 12 December 2023 • Accepted: 28 May 2024 •
Published Online: 17 June 2024

Andrea Annunziata,[1,2,3] Luise Becker,[3] Marta L. Murillo-Sánchez,[3] Patrick Friebel,[3] Salvatore Stagira,[1,2] Davide Faccialà,[2] Caterina Vozzi,[2] and Laura Cattaneo[3,a)]

AFFILIATIONS

[1] Department of Physics, Politecnico di Milano, Milano, Italy
[2] Istituto di Fotonica e Nanotecnologie-CNR (CNR-IFN), 20133 Milano, Italy
[3] Max-Planck-Institut für Kernphysik, Saupfercheckweg 1, D-69117 Heidelberg, Germany

[a)] **Author to whom correspondence should be addressed:** laura.cattaneo@mpi-hd.mpg.de. **URL:** https://www.mpi-hd.mpg.de/mpi/de/forschung/abteilungen-und-gruppen/unabhaengige-forschungsgruppen/ulcd

ABSTRACT

Thermotropic liquid crystals are versatile optical materials that exhibit a state of matter intermediate between liquids and solids. Their properties can change significantly with temperature, pressure, or other external factors, leading to different phases. The transport properties within these materials in different phases are still largely unexplored, and their understanding would enable exciting prospects for innovative technological advancements. High-order harmonic spectroscopy proved to be a powerful spectroscopic tool for investigating the electronic and nuclear dynamics in matter. Here, we report the first experimental observation of high-order harmonic generation in thermotropic liquid crystals in two different phase states, nematic and isotropic. We found the harmonic emission in the nematic phase to be strongly dependent on the relative orientation of the driving field polarization with respect to the liquid crystal alignment. Specifically, the harmonic yield has a maximum when the molecules are aligned perpendicularly to the polarization of the incoming radiation. Our results establish the first step for applying high-order harmonic spectroscopy as a tool for resolving ultrafast electron dynamics in liquid crystals with unprecedented temporal and spatial resolution.

I. INTRODUCTION

With the increasing need for energy-efficient technologies for batteries or transistors, liquid crystals (LCs), notoriously used for displays or tunable optical elements (photonic crystals[1] or q-plates,[2,3]), proved to be a promising platform for electron and ion transport, combining self-assembly, stimuli response, self-healing, and easy processability.[4,5] Over the past two decades, this led to a significant effort devoted to designing new LC molecules with high mobility that may become competitive candidates for organic semiconductor applications, such as organic light emitting diodes, organic field effect transistors, or organic solar cells.[5–8] Although significant progress has been made in chemical synthesis and molecular design to improve transport dynamics in organic materials, some challenges have yet to be overcome for its practical implementation.[9] Among them is the lack of a detailed understanding, both experimental and theoretical, of the electronic and coupled intra-to-inter-molecular dynamics upon charge-transfer phenomena.[9,10]

The electronic excitation of LCs has been the subject of multiple research studies, in particular concerning the absorption and fluorescence activity of alkylbiphenyl-based LC molecules (nCB), when diluted in suitable solvents.[11–13] Of particular interest is the fact that these molecules, within the LC mesophase, pair up in excimers, when UV-excited (involving a conformational change),[14,51] and dimers in anti-parallel configuration.[15,16] The presence of such dimeric building blocks and the connected electron–nuclear dynamic, their geometrical arrangement, formation over time, and connection to the LC nature is still a topic of investigation.[14–16,51] Moreover, studies on the time-resolved ultrafast dynamics in LCs revealed the possibility of exploiting the optical Kerr effect in the isotropic LCs reaching time scales in the order of ~100 ps,[17–20] going down up to ~500 fs in the nematic phase,[21] but there is still lack of time-resolved studies on a ultrafast timescale involving the electronic excitation of LCs.

In this framework, high-order harmonic generation (HHG) spectroscopy revealed to be a valuable approach for studying electron and nuclear dynamics in multiple molecular targets.[22–26] In

the well-established description of HHG in gases, high-order harmonics are generated when an intense laser pulse is focused on the gas medium. Due to the strong non-linear interaction, an electron can be freed by tunnel ionization and then accelerated by the external electric driving field. The electron may then recombine with the parent ion. The burst of light released upon recollision is composed of photons having energies going up to several tens of electronvolts with attosecond duration.[27,28] Each emitted photon energy is linked directly to a well-defined temporal interval from the ionization to the recombination of the electron, providing an extremely detailed snapshot of the structure of the system under investigation.[22,24,25,29,30] In this highly non-linear regime, the material response to the external electric field deviates from being described by its electric susceptibility. Thus, the relative intensity between each harmonic does not decrease exponentially with the order.

The extension of HHG spectroscopy to solids opened the way for all-optical characterization techniques, such as band structure reconstruction,[31] Berry phase measurement,[32] and strong-field-induced band structure dynamics.[33] Recently, Luu *et al.* demonstrated the possibility of generating high-order harmonics from water and the most common alcohols. The generated spectra are very sensitive to the density of states and bandgaps, establishing the potential of HHG spectroscopy to investigate the electronic structure of liquids.[34,35]

In the context of HHG, LCs are a special class of materials because, despite their liquid-like macroscopic appearance, they have a well-defined and controllable symmetry, orientation, periodicity, and a low ionization potential well-below 10 eV.[36] Harmonic generation in LCs in the perturbative regime has already been observed,[37,38] demonstrating the capability of non-linear spectroscopy for studying the LCs alignment and extracting non-linear polarizability.[39,40] To the best of our knowledge, the generation of harmonics in LCs in the non-perturbative regime has not been investigated yet.

In this manuscript, we report the first experimental observation of HHG from thermotropic LCs, where phase transitions are triggered by temperature changes. This work is intended to be the first in a series sharing the common goal of bridging the gap of knowledge about coupled electron–nuclear dynamics in LC systems, a fundamental aspect for future applications as charge transport materials. In particular, we investigated nematic and isotropic mesophases. In the nematic mesophase [Fig. 1(a)], the LC molecules lack translational symmetry, but they display macro-domains with well-defined orientational symmetry, resulting in a peaked molecular distribution oriented along a specific direction ($\hat{n}$) called director [orange arrow shown in Fig. 1(a)]. The application of an external electric field allows the orientations of all the directors of the macro-domains along the electric field lines. On the other hand, in the isotropic mesophase [Fig. 1(b)], the molecules are randomly oriented.

We generated high-order harmonic radiation in three different LCs driving the process with a strong mid-IR laser pulse centered at 3.8 μm, and we characterized the harmonic emission as a function of the driving field polarization direction. The wavelength was selected to be out of resonance for all the LCs under examination, thereby mitigating potential damages induced by direct electronic excitation at the intensities employed during the experiment. To

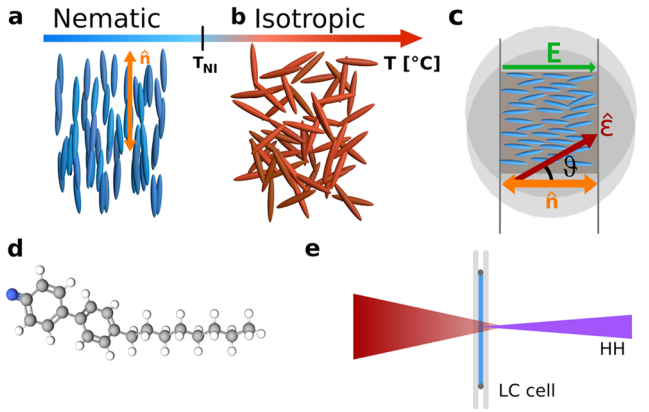

FIG. 1. (a) LCs in the nematic phase, where the molecules are aligned along an average direction ($\hat{n}$, orange arrow). (b) LCs in the isotropic phase, where the molecules are randomly oriented. T_{NI} on the arrow below indicates the nematic to isotropic transition temperature. (c) Lab-made cell used to contain the LCs sample. The director n represents the molecular average alignment direction (orange arrow) and follows the external AC field. The driving field polarization direction $\hat{\varepsilon}$ is considered with respect to $\hat{n}$, corresponding to the horizontal direction in the laboratory frame. (d) Graphical depiction of the 8CB molecule. (e) Schematic of the interaction region seen from the top. The red beam represents the driving field, which is focused ~1 mm after the LC cell. The LCs inside the cell are depicted in light blue. In violet (HH), there are the emitted harmonics from the LCs.

prevent unwanted phase transitions and damages in the LC cells, the laser repetition rate was reduced to 10 Hz using a chopper. The laser focus was placed ~1 mm after the sample [Fig. 1(e)], resulting in a beam waist at the interaction region of ~100 μm. Our observations revealed a strong dependence of the HHG emission on the relative orientation between the driving field polarization direction and the director of the LC molecules in the nematic phase. We show how the orientation of the director is preserved during the strong-field interaction even at intensities of the order of ~ 10^{12} W/cm^2, which are needed for driving the HHG process, and how this orientation directly affects the efficiency of the process itself. This work constitutes a first step in understanding the ultrafast electron dynamics in LCs, elucidating the intricate interplay between the electronic and molecular dynamics associated with each specific mesophase.

II. RESULTS

We performed the experiments using three LCs: 8CB (4-cyano-4′-octylbiphenyl), 8OCB (4-cyano-4-n-oxyoctyl-biphenyl), and E7, which is a mixture of 5CB (4-cyano-4′-n-pentyl-biphenyl, 51%), 7CB (4-Heptyl-4-biphenylcarbonitrile, 25%), 8OCB (16%), and 5CT (4-cyano-4-n-pentyl-p-terphenyl, 8%). LCs were exposed to the laser beam (P-polarized, centered at the wavelength of 3.8 μm) either as contained in lab-made cells [sketch shown in Fig. 1(c)] or free-standing thin films. In this case, we only used 8CB among the three LCs investigated here since it is the only one providing sufficient surface tension to form a stable film over time. Details about the experimental setup, free-standing film formation, cell preparation, and temperature stabilization can be found in the supplementary material.

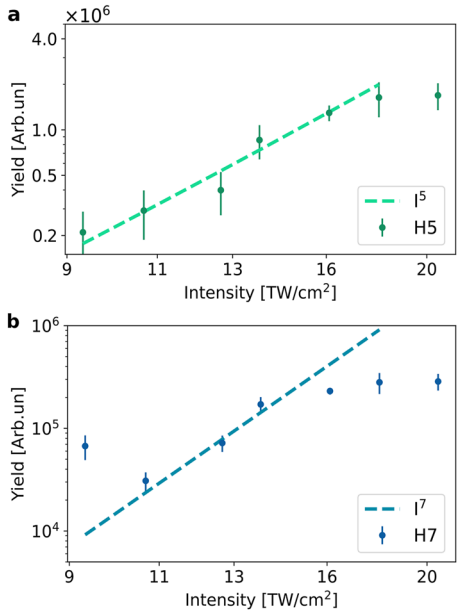

FIG. 2. Yield of the fifth harmonic (a) and the seventh harmonic **b**) as a function of the driving field intensity for a thin film of 8CB. Both axes are in the $\log_{10}$ scale. The experimental data (triangles) are superimposed on the power law in the same order as the emitted harmonic (dashed lines).

A. Harmonics intensity dependence

We first performed an intensity scan in a free-standing film of 8CB at room temperature (20 °C) to assess the non-perturbative nature of the observed harmonic emission. At this temperature, 8CB is in the smectic A phase. Here, the molecules maintain the general order observed in the nematic phase but also align themselves in distinct layers. We kept this temperature because the 8CB film formed in the smectic A phase exhibits greater stability compared to the nematic phase. This ensures the preservation of the molecules' ability to pair up in dimers, without compromising the local order probed by the HHG mechanism.

Figure 2 shows the intensity of the fifth (a) and seventh (b) harmonic as a function of the driving field intensity in the $\log_{10}$ scale. The green (blue) triangles represent the experimental data obtained for H5 (H7), whereas the dashed lines show the expected behavior in the perturbative regime. For driving field intensity up 16 TW/cm^2, the harmonics scaling is clearly perturbative, while above this value, a saturation of the emitted harmonics is observed, indicating the non-perturbative origin of the HHG process.

To perform HHG experiments across all LC mesophases and different alignment configurations, the LC-filled cells were preferred compared to the free-standing film. The latter survives only within a limited range of temperature (below 33 °C) and only provides a specific LC orientation, where the long molecular axis is aligned perpendicular to the film surface. This would have prevented the observation of the harmonic responses as a function of the polarization direction, since the driving field will always be orthogonal to the uniform short molecular axis.

B. Harmonics generation in the nematic phase

Moving to the LC cells, we analyzed the harmonic emission from E7, 8CB, and 8OCB in the nematic phase by setting the temperature below the transition temperature to the isotropic phase (60, 40.5, and 80 °C, respectively).

For all the LCs under investigation, the harmonics were collected as a function of the relative orientation between the applied external field and the (linear) driving field polarization direction. This orientation was identified by the angle θ, which was varied using a half wave-plate, in steps of 8°.

The laser intensity was tuned to avoid unwanted phase transitions and degradation of the sample during the measurement. At the focus, the peak intensity of the driving field was estimated on the order of 26 TW/cm^2 for E7, 21 TW/cm^2 for 8CB, and 18 TW/cm^2, for 8OCB. Possible reorientation of molecular alignment due to such strong fields can be neglected since harmonic emission occurs within half-cycles of the driving field (corresponding to ~6 fs), while molecular reorientation takes place on time scales several orders of magnitude longer than those of high harmonic generation (HHG) and the pulse duration.

Figure 3 shows the yield of the detected harmonics as a function of the laser polarization direction θ for (a) E7, (b) 8CB, and (c) 8OCB. For $\theta = 0°$ and 180°, the driving field is aligned parallel to the AC field, while for $\theta = \pm 90°$, the driving field is aligned perpendicular to the AC field. We refer to these two cases as *parallel* and *perpendicular* configurations, respectively. For all the harmonics, the yield is normalized to the maximum, and only odd-order harmonics were detected.

For E7 and 8CB, the third, fifth, and seventh harmonics (H3, H5, and H7) were observed during the polarization scan. In 8OCB, only H3 and H5 were collected because of the lower driving field intensity used. For all three LCs examined, we attribute the absence of higher-order harmonics to the scattering occurring within the LC bulk, which increases as a function of the photon energy, together with additional losses due to multiple reflections at the substrates interfaces. Increasing the driving field intensity enabled the observation of harmonics up to the ninth order. However, the resulting stability of the harmonics was insufficient for reliable measurements.

In all three samples, all the harmonics showed maximum yield in the perpendicular configuration ($\theta = \pm 90°$), giving rise to a twofold symmetry in the polar plots. The yield then quickly drops as we depart from the perpendicular configuration, producing two distinctive lobes. In particular, we observe that the width of these lobes decreases by increasing the harmonic order for all the LCs under investigation. Moreover, distinct weaker lobes are observed for H3 in the parallel configuration ($\theta = 0°$ and 180°). The intensity of these weak lobes relative to the main ones is 8.5%, 15%, and 18% for E7, 8CB, and 8OCB, respectively. For higher-order harmonics, the emission in the parallel configuration drastically drops to the background level, resulting in a non-detectable intensity. This experimental observation is in good qualitative agreement with the theoretical calculation of Lü and Bian for sub-gap harmonics in a liquid-crystal-like model.[41]

The harmonic yield as a function of the driving field polarization direction has been compared to a simple perturbative model to extract information about the local order of the LCs under inves-

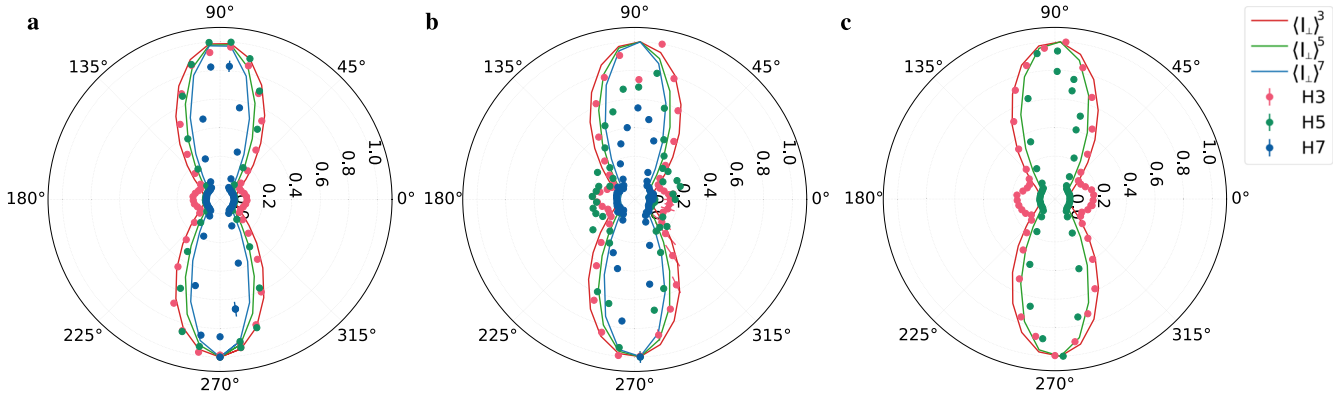

FIG. 3. Normalized intensity of the emitted harmonics in the nematic phase for (a) E7, (b) 8CB, and (c) 8OCB as a function of the polarization direction at 36, 36, and 74 °C, respectively. $\langle I_\perp \rangle$ is the distribution obtained by the fitting procedure (solid lines) raised to the same power as the emitted harmonic.

tigation. Considering an ensemble of molecules having a Gaussian distribution of their long molecular axis around the director $\hat{n}$, we determine the full-width half maximum of the distribution to get typical values of the order parameter S found in the literature, which are 0.7, 0.5, and 0.6 for E7, 8CB, and 8OCB respectively.[42–44]

Assuming an ideal emitter, where the emitted field is maximum with a driving field perpendicular to the long molecular axis, we got an intensity distribution $\langle I_\perp \rangle$, which is a function of the angle θ. Subsequently, $\langle I_\perp \rangle$ is then raised to the order of the harmonic with which it is compared. The details about the derivation of the order parameter and the retrieval of $\langle I_\perp \rangle$ can be found in Sec. III of the SM. For all the LCs under investigation, the retrieved intensity distribution for H3 (Fig. 3, $\langle I_\perp \rangle^3$) is in good qualitative agreement with the experimental data. This would indicate the perturbative origin of H3 since the intensity profile of the emitted harmonic scales with the third power. For higher-order harmonics, discrepancies between the obtained distribution ($\langle I_\perp \rangle^5$, and $\langle I_\perp \rangle^7$) start to be evident, becoming higher as the harmonic order increases, suggesting that the underlying emission mechanism cannot be simply interpreted with our perturbative model.

C. Harmonics generation in the isotropic phase

For each LC under study, right after measuring the nematic phase, we switched off the applied voltage, heated the sample above the nematic-to-isotropic transition temperature, and characterized the HHG emission in the isotropic phase, keeping the same driving field intensity as in the nematic phase. Figure 4 shows the HHG response in (a) E7, (b) 8CB, and (c) 8OCB as a function of the laser polarization direction in the isotropic phase at temperatures of 80, 90, and 100 °C, respectively. We expect the LC molecules to be randomly aligned and, therefore, the polarization direction of the driving field should not affect the efficiency of the HHG process. The results indeed show a weaker dependence of the HHG intensity with the polarization angle, particularly for H3. A residual modulation can be observed for higher orders, even if not as pronounced

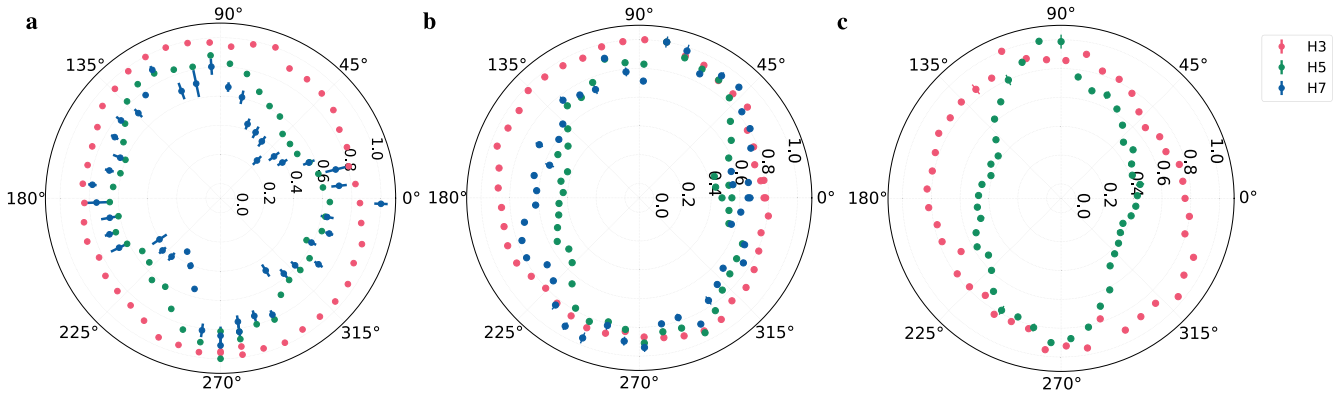

FIG. 4. Normalized intensity of the emitted harmonics in the isotropic phase for (a) E7, (b) 8CB, and (c) 8OCB as a function of the polarization direction at 36, 36, and 74 °C, respectively.

as in the nematic phase, with a preferential emission in the perpendicular configuration. We attribute this residual modulation to the persistence of partial alignment induced by the contact with the cell substrates. Indeed, even in the isotropic phase, surface effects dominate, favoring a specific anchoring of the neighboring molecules to the CaF_2 substrate, which imposes a residual alignment. This, in turn, modulates the emitted harmonics as a function of the driving field polarization direction.

III. DISCUSSION

To further investigate the origin of the high yield obtained in the nematic phase aligned in the perpendicular configuration, we compared the HHG spectra obtained in the two phases in this configuration. We focused our attention on E7, which, being specifically designed for display applications, is the most stable in terms of nematic-temperature range (−60 to 60 °C) and a more efficient alignment with the external AC field (no surface treatments were used in the prepared LC cells). Figure 5 presents a comparison of the spectra in both cases, along with the overall enhancement observed when transitioning from the isotropic to the aligned nematic phase. The harmonics generated in the aligned nematic phase are significantly more intense than the ones obtained in the isotropic phase, with the harmonic yield monotonically increasing as a function of the harmonic order. In the nematic phase, a redshift is also observed compared to the isotropic phase for all the harmonics. Specifically, the shifts are 10 nm for H3, 13 nm for H5, and 10 nm for H7. The origin of this redshift may be attributed to a non-negligible nuclear motion during the HHG process.[45,46] This phenomenon is usually related to higher ionization rates and smaller ionization potential under a photodissociation process[45,47–49] or to intermediate transitions during the HHG.[50] To properly understand this observation, numerical calculations are needed.

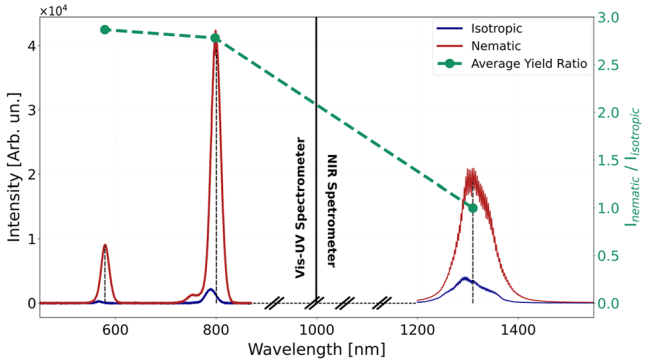

FIG. 5. Harmonic response in the isotropic (blue) and nematic (red) phases for the same polarization direction of the driving field in E7. The harmonics in the visible and near-infrared ranges were acquired with two different spectrometers. Due to the absence of overlapping regions, it is not possible to compare the relative intensities between the NIR and vis–UV ranges. The green circles (right axis) represent the total yield ratio averaged over all possible polarization directions with respect to the molecular alignment between the measured intensity for the nematic and isotropic phases. A redshift for all the harmonic order is also observed, represented by the black dashed lines.

Next, we discuss the origin of the high HHG yield observed in the nematic phase compared to the isotropic phase. This could be attributed to several effects. Let us assume that the HHG emission comes from an ensemble of molecules, each considered as an ideal emitter, namely, only the driving field projection orthogonal to the long molecular axis contributes to the emission. If we disregard macroscopic phase matching effects, we expect a higher yield from the aligned nematic phase in the perpendicular configuration as compared to the isotropic phase. Indeed, in the aligned nematic phase, all molecules are aligned along the axis that maximizes HHG, and they all contribute to the HHG process with the same yield. In contrast, in the isotropic phase, molecules are randomly oriented compared to the driving field polarization direction, resulting in a reduced or negligible contribution from molecules that are not aligned perpendicularly to the driving field.

On the other hand, coherence effects could also influence the HHG mechanism (supplementary material, Sec. IV). To understand the relative impact of the coherence effects on the observed enhancement, we averaged the HHG emission over all the possible orientations of the driving field polarization direction in both nematic and isotropic phases. Calling $I_N(\theta)$, the detected Nth harmonic intensity for a driving field polarization direction θ, this integral reads

$$\pi \int_0^{2\pi} I_N(\theta) \sin(\theta)\, d\theta. \tag{1}$$

We numerically evaluated the average yield for both the nematic and isotropic phases. Then, we computed the ratio for all the observed harmonics, and the results are shown with green circles (right axis) in Fig. 5. If there are no coherence effects affecting the HHG emission, the ratio between the average nematic and average isotropic HHG yield should be equal to one. For H3, the experimental results suggest that the observed enhancement in the perpendicular configuration cannot be attributed to coherence effects but rather to the alignment effect. However, this is not the case for H5 and H7, thus the enhancement must originate from either the macroscopic collective coherent response of the aligned LCs or from a change in the microscopic HHG response in the two different phases of the LCs.

As previously mentioned, it has been identified that nCB (and nCOB[12]) molecules form dimeric clusters $(nCB)_2$, which imposes a reduced inter-molecular distance (below 4 Å) and a defined antiparallel configuration to the involved molecular units in a diluted solution of different solvents.[14–16,51] In particular, the dimeric contribution becomes dominant at high concentrations up to the neat phase.[11–13,15] When looking at the fluorescence spectra of pure 8CB at different temperatures, the dimer/excimer contribution is dominant in the nematic and smectic phase, and it becomes equally shared with the monomeric contribution in the isotropic phase and almost negligible in the crystalline phase where almost pure monomeric emission is observed.[11] In our case, we could think that the observed enhanced emission in the nematic phase is the result of two factors: (I) the presence of dimeric clusters favoring a larger delocalization of the excited electron wave-packet thanks to the coupling of the two biphenyl groups almost irrespective of the alkyl/alkoxy chain; (II) the alignment over the entire bulk of such

dimeric units, which amplify the efficiency of the triggered process, particularly this happens when the incoming radiation is polarized perpendicular to the LC director, and most probably, along the direction where the electron density of the highest occupied molecular orbital (HOMO) is greater. On the other hand, in the isotropic phase, the reduced and isotropic response can be attributed to the reduced concentration of dimeric clusters and their lack of alignment.

To find evidence of our interpretation, it is essential to conduct a direct quantitative comparison between our experimental results and theoretical calculations. This would allow us to clarify the mechanism behind the non-perturbative HHG emission and to identify possible additional transport mechanisms involving hopping/delocalization among neighboring dimers. Finally, phase-matching could also contribute as an additional possible source of the observed average yield enhancement.

IV. CONCLUSION

In this study, we report the first experimental observation of high-order harmonic generation in the non-perturbative regime from three different thermotropic LCs. The harmonic emission as a function of the driving field polarization direction has been characterized within both the aligned nematic and isotropic mesophases.

Our experimental observations reveal a strong dependence of the harmonic emission on the LC phase. Indeed, a strong modulation of the harmonic emission was observed by changing the polarization direction of the driving field in the nematic phase, with a strong enhancement when the driving field was orthogonally polarized to the director and a clear suppression when the driving field was parallel. In contrast, the harmonic response in the isotropic phase exhibited a more uniform dependence on the driving field polarization direction.

Moreover, the harmonic yield showed a significant enhancement in the nematic phase compared to the isotropic phase. Our analysis showed that the observed enhancement cannot be solely attributed to the molecular alignment for the harmonics above the third order. We argue this result considering the presence of aligned anti-parallel dimeric clusters. The dimeric configuration favors the delocalization of the electronic wave function around the coupled biphenyl groups. In particular, the observed enhanced HHG emission indicates a perpendicular spatial distribution of the HOMO wave function compared to the molecular/dimer orientation. The overall alignment of all dimers within the bulk increases the efficiency of the HHG process, fixing the relative geometry between the polarization of the incoming radiation and the emitting units. In conclusion, HHG is confirmed to be a powerful investigation tool sensitive to the local order in a soft matter system. Moreover, it is particularly adept at identifying the critical factors that lead to the formation of delocalized states. This is a critical aspect for understanding long-range transport processes in soft matter and harnessing them for future technological applications. This work represents a first step in understanding the ultrafast dynamics in LCs, unfolding the complexity of the electron and molecular dynamics ruling each mesophase at unprecedented spatial and temporal scales. Moreover, since their temperature controlled the mesophase nature, thus the possibility to go from an oriented and periodic structure to a fully random system, LCs will serve as ideal benchmark materials to bridge molecular and solid-state high-order harmonic generation exploiting phase transitions.

SUPPLEMENTARY MATERIAL

The supplementary material includes details on the cell preparation, the experimental setup for generating high-order harmonics, the modeling used in Fig. 3, the integration over the driving field polarization direction, and finally, a list of pseudo-color plots of the raw data.

ACKNOWLEDGMENTS

L.C. acknowledges the Max Planck Group Leader program for funding her independent research.

This publication is based upon work from COST Action Attochem Grant No. CA18222, supported by COST (European Cooperation in Science and Technology).

C.V., D.F., and A.A. acknowledge the funding through the MIUR PRIN CONQUEST (Grant No. 2020JZ5N9M).

AUTHOR DECLARATIONS

Conflict of Interest

The authors have no conflicts to disclose.

Author Contributions

Andrea Annunziata: Data curation (equal); Formal analysis (lead); Investigation (equal); Methodology (equal); Writing – original draft (lead); Writing – review & editing (equal). **Luise Becker**: Data curation (equal); Investigation (equal). **Marta L. Murillo-Sánchez**: Writing – original draft (equal); Writing – review & editing (equal). **Patrick Friebel**: Writing – original draft (equal); Writing – review & editing (equal). **Salvatore Stagira**: Supervision (equal); Validation (equal); Writing – original draft (equal); Writing – review & editing (equal). **Davide Faccialà**: Supervision (equal); Validation (equal); Writing – original draft (equal); Writing – review & editing (equal). **Caterina Vozzi**: Supervision (equal); Validation (equal); Writing – original draft (equal); Writing – review & editing (equal). **Laura Cattaneo**: Conceptualization (lead); Data curation (equal); Formal analysis (supporting); Funding acquisition (lead); Investigation (equal); Methodology (equal); Project administration (lead); Supervision (equal); Validation (equal); Writing – original draft (equal); Writing – review & editing (equal).

DATA AVAILABILITY

The data that support the findings of this study are available from the corresponding author upon reasonable request.

REFERENCES

[1] S. H. Ryu, M.-J. Gim, W. Lee, S.-W. Choi, and D. K. Yoon, "Switchable photonic crystals using one-dimensional confined liquid crystals for photonic device application," ACS Appl. Mater. Interfaces **9**, 3186–3191 (2017).

[2] L. Marrucci, C. Manzo, and D. Paparo, "Optical spin-to-orbital angular momentum conversion in inhomogeneous anisotropic media," Phys. Rev. Lett. **96**, 163905 (2006).

[3] E. Karimi, B. Piccirillo, E. Nagali, L. Marrucci, and E. Santamato, "Efficient generation and sorting of orbital angular momentum eigenmodes of light by thermally tuned q-plates," Appl. Phys. Lett. **94**, 231124 (2009).

[4] J. Uchida, B. Soberats, M. Gupta, and T. Kato, "Advanced functional liquid crystals," Adv. Mater. **34**, 2109063 (2022).

[5] T. Kato, M. Yoshio, T. Ichikawa, B. Soberats, H. Ohno, and M. Funahashi, "Transport of ions and electrons in nanostructured liquid crystals," Nat. Rev. Mater. **2**, 17001 (2017).

[6] H. Iino, T. Usui, and J.-i. Hanna, "Liquid crystals for organic thin-film transistors," Nat. Commun. **6**, 6828 (2015).

[7] J.-i. Hanna, A. Ohno, and H. Iino, "Charge carrier transport in liquid crystals," Thin Solid Films **554**, 58–63 (2014), 10th International Conference on Nano-Molecular Electronics (ICNME2012).

[8] R. Termine and A. Golemme, "Charge mobility in discotic liquid crystals," Int. J. Mol. Sci. **22**, 877 (2021).

[9] G. Schweicher, G. Garbay, R. Jouclas, F. Vibert, F. Devaux, and Y. H. Geerts, "Molecular semiconductors for logic operations: Dead-end or bright future?," Adv. Mater. **32**, 1905909 (2020).

[10] A. Troisi, "Charge transport in high mobility molecular semiconductors: Classical models and new theories," Chem. Soc. Rev. **40**, 2347–2358 (2011).

[11] D. Baeyens-Volant and C. David, "Energy transfer and migration in liquid crystalline systems. II–4-Octyl-4′-Cyanobiphenyl, 1 -Heptyl-4-(4′-Cyanophenyl) cyclohexane and 4-pentyl-4′-methylbiphenyl," Mol. Cryst. Liq. Cryst. **116**, 217–243 (1985).

[12] C. David and D. Baeyens-volant, "Energy transfer and migration in liquid crystalline 4-cyano 4-alkoxybiphenyls," Mol. Cryst. Liq. Cryst. **106**, 45–65 (1984).

[13] C. David and D. Baeyens-volant, "Absorption and fluorescence spectra of 4-cyanobiphenyl and 4′-alkyl- or 4′-alkoxy-substituted liquid crystalline derivatives," Mol. Cryst. Liq. Cryst. **59**, 181–196 (1980).

[14] A. Klock, W. Rettig, J. Hofkens, M. Van Damme, and F. De Schryver, "Excited state relaxation channels of liquid-crystalline cyanobiphenyls and a ring-bridged model compound. comparison of bulk and dilute solution properties," J. Photochem. Photobiol., A **85**, 11–21 (1995).

[15] S. Takabatake and T. Shikata, "Evidence of anti-parallel dimer formation of 4-cyano-4-alkyl biphenyls in isotropic cyclohexane solution," Phys. Chem. Chem. Phys. **17**, 1934–1942 (2015).

[16] C. Amovilli, I. Cacelli, S. Campanile, and G. Prampolini, "Calculation of the intermolecular energy of large molecules by a fragmentation scheme: Application to the 4-n-pentyl-4- cyanobiphenyl (5CB) dimer," J. Chem. Phys. **117**, 3003–3012 (2002).

[17] F. W. Deeg, S. R. Greenfield, J. J. Stankus, V. J. Newell, and M. D. Fayer, "Nonhydrodynamic molecular motions in a complex liquid: Temperature dependent dynamics in pentylcyanobiphenyl," J. Chem. Phys. **93**, 3503–3514 (1990).

[18] S. D. Gottke, H. Cang, B. Bagchi, and M. D. Fayer, "Comparison of the ultrafast to slow time scale dynamics of three liquid crystals in the isotropic phase," J. Chem. Phys. **116**, 6339–6347 (2002).

[19] H. Cang, J. Li, V. N. Novikov, and M. D. Fayer, "Dynamics in supercooled liquids and in the isotropic phase of liquid crystals: A comparison," J. Chem. Phys. **118**, 9303–9311 (2003).

[20] N. T. Hunt, A. A. Jaye, and S. R. Meech, "Ultrafast dynamics in complex fluids observed through the ultrafast optically-heterodyne-detected optical-kerr-effect (OHD-OKE)," Phys. Chem. Chem. Phys. **9**, 2167–2180 (2007).

[21] L. Cattaneo, M. Savoini, I. Muševič, A. Kimel, and T. Rasing, "Ultrafast all-optical response of a nematic liquid crystal," Opt. Express **23**, 14010–14017 (2015).

[22] J. P. Marangos, "Development of high harmonic generation spectroscopy of organic molecules and biomolecules," J. Phys. B: At., Mol. Opt. Phys. **49**, 132001 (2016).

[23] H. Niikura, N. Dudovich, D. M. Villeneuve, and P. B. Corkum, "Mapping molecular orbital symmetry on high-order harmonic generation spectrum using two-color laser fields," Phys. Rev. Lett. **105**, 053003 (2010).

[24] J. Itatani, J. Levesque, D. Zeidler, H. Niikura, H. Pépin, J. C. Kieffer, P. B. Corkum, and D. M. Villeneuve, "Tomographic imaging of molecular orbitals," Nature **432**, 867–871 (2004).

[25] C. Vozzi, M. Negro, F. Calegari, G. Sansone, M. Nisoli, S. De Silvestri, and S. Stagira, "Generalized molecular orbital tomography," Nat. Phys. **7**, 822–826 (2011).

[26] E. Luppi and E. Coccia, "Role of inner molecular orbitals in high-harmonic generation spectra of aligned uracil," J. Phys. Chem. A **127**, 7335–7343 (2023).

[27] P. B. Corkum, "Plasma perspective on strong field multiphoton ionization," Phys. Rev. Lett. **71**, 1994–1997 (1993).

[28] M. Lewenstein, P. Balcou, M. Y. Ivanov, A. L'Huillier, and P. B. Corkum, "Theory of high-harmonic generation by low-frequency laser fields," Phys. Rev. A **49**, 2117–2132 (1994).

[29] A. Camper, A. Ferré, V. Blanchet, D. Descamps, N. Lin, S. Petit, R. Lucchese, P. Salières, T. Ruchon, and Y. Mairesse, "Quantum-path-resolved attosecond high-harmonic spectroscopy," Phys. Rev. Lett. **130**, 083201 (2023).

[30] T. Okino, Y. Furukawa, Y. Nabekawa, S. Miyabe, A. Amani Eilanlou, E. J. Takahashi, K. Yamanouchi, and K. Midorikawa, "Direct observation of an attosecond electron wave packet in a nitrogen molecule," Sci. Adv. **1**, e1500356 (2015).

[31] G. Vampa, T. J. Hammond, N. Thiré, B. E. Schmidt, F. Légaré, C. R. McDonald, T. Brabec, D. D. Klug, and P. B. Corkum, "All-optical reconstruction of crystal band structure," Phys. Rev. Lett. **115**, 193603 (2015).

[32] T. T. Luu and H. J. Wörner, "Measurement of the berry curvature of solids using high-harmonic spectroscopy," Nat. Commun. **9**, 916 (2018).

[33] A. J. Uzan-Narovlansky, Á. Jiménez-Galán, G. Orenstein, R. E. F. Silva, T. Arusi-Parpar, S. Shames, B. D. Bruner, B. Yan, O. Smirnova, M. Ivanov, and N. Dudovich, "Observation of light-driven band structure via multiband high-harmonic spectroscopy," Nat. Photonics **16**, 428–432 (2022).

[34] T. T. Luu, Z. Yin, A. Jain, T. Gaumnitz, Y. Pertot, J. Ma, and H. J. Wörner, "Extreme–ultraviolet high–harmonic generation in liquids," Nat. Commun. **9**, 3723 (2018).

[35] Y. H. Kim, H. Kim, S. C. Park, Y. Kwon, K. Yeom, W. Cho, T. Kwon, H. Yun, J. H. Sung, S. K. Lee, T. T. Luu, C. H. Nam, and K. T. Kim, "High-harmonic generation from a flat liquid-sheet plasma mirror," Nat. Commun. **14**, 2328 (2023).

[36] D. Sharma and S. Tiwari, "Comparative computational analysis of electronic structure, MEP surface and vibrational assignments of a nematic liquid crystal: 4-n-methyl-4′-cyanobiphenyl," J. Mol. Liq. **214**, 128–135 (2016).

[37] S. I. Trashkeev, N. T. Vasenin, S. M. Vatnik, I. A. Vedin, A. V. Ivanenko, and V. M. Klementyev, "Harmonic generation in a nematic liquid crystal," Laser Phys. Lett. **17**, 075002 (2020).

[38] I. Freund and P. M. Rentzepis, "Second-harmonic generation in liquid crystals," Phys. Rev. Lett. **18**, 393–394 (1967).

[39] M. B. Feller, W. Chen, and Y. R. Shen, "Investigation of surface-induced alignment of liquid-crystal molecules by optical second-harmonic generation," Phys. Rev. A **43**, 6778–6792 (1991).

[40] K. Y. Wong and A. F. Garito, "Third-harmonic-generation study of orientational order in nematic liquid crystals," Phys. Rev. A **34**, 5051–5058 (1986).

[41] L.-J. Lü and X.-B. Bian, "High-order harmonic generation in a liquid-crystal-like model," Phys. Rev. A **108**, 013504 (2023).

[42] B. Bahadur, R. K. Sarna, and V. G. Bhide, "Refractive indices, density and order parameter of some technologically important liquid crystalline mixtures," Mol. Cryst. Liq. Cryst. **72**, 139–145 (1982).

[43] C. D. Southern and H. F. Gleeson, "Using the full Raman depolarisation in the determination of the order parameters in liquid crystal systems," Eur. Phys. J. E **24**, 119–127 (2007).

[44]D. Bauman and E. Wolarz, "Study of orientational order of liquid crystal 8 OCB doped with perylene-like dyes by means of polarized optical spectroscopy," Z. Naturforsch. A **51**, 1192–1196 (1996).
[45]X.-B. Bian and A. D. Bandrauk, "Probing nuclear motion by frequency modulation of molecular high-order harmonic generation," Phys. Rev. Lett. **113**, 193901 (2014).
[46]C. P. Zhang, C. L. Xia, and X. Y. Miao, "High-order harmonic generation from molecular ions in the coherent electronic states," Europhys. Lett. **126**, 23001 (2019).
[47]T. Zuo and A. D. Bandrauk, "Charge-resonance-enhanced ionization of diatomic molecular ions by intense lasers," Phys. Rev. A **52**, R2511–R2514 (1995).
[48]M. Lara-Astiaso, R. E. F. Silva, A. Gubaydullin, P. Rivière, C. Meier, and F. Martín, "Enhancing high-order harmonic generation in light molecules by using chirped pulses," Phys. Rev. Lett. **117**, 093003 (2016).
[49]S. Yue, S. Fu, J. Li, X. Zhang, Y. Feng, B. Hu, and H. Du, "A redshift mechanism of high-order harmonics: Change of ionization energy," J. Chem. Phys. **148**, 234304 (2018).
[50]X.-B. Bian and A. D. Bandrauk, "Spectral shifts of nonadiabatic high-order harmonic generation," Appl. Sci. **3**, 267–277 (2013).
[51]Y. P. Piryatinskiĭ and O. V. Yaroshchuk, "Photoluminescence of pentyl-cyanobiphenyl in liquid-crystal and solid-crystal states," Opt. Spectrosc. **89**, 860–866 (2000).